

2850 W. Bayshore Road Palo Alto, California 94303-3843 (650) 494-7351

**Properties of Viscoelastic
Materials Under
Centrifugal Loads**

Submitted to:

DISTRIBUTION STATEMENT A
Approved for Public Release
Distribution Unlimited

19990406 031

2850 W. Bayshore Road Palo Alto, California 94303-3843 (650) 494-7351 Fax: (650) 494-8749

**Properties of Viscoelastic
Materials Under
Centrifugal Loads**

Submitted to:

**Wright Labs
Wright-Patterson AFB, OH**

**Report No. 98-02-01
February 1998**

DISTRIBUTION STATEMENT A
Approved for Public Release
Distribution Unlimited

DTIC QUALITY INSPECTED 2

Contents

| | |
|--|-----------|
| 1. Properties of Viscoelastic Materials Under Centrifugal Loads | 1 |
| 1.1 Summary | 1 |
| 1.2 Introduction | 1 |
| 1.3 Material Considerations | 2 |
| 1.3.1 Interfacial Slip | 6 |
| 1.3.2 Poker Chip | 8 |
| 1.3.3 Complex Shear Modulus | 8 |
| 1.3.4 PVT Data and Analysis | 9 |
| 1.4 Experimental Blade Design | 13 |
| 1.4.1 Thermal Expansion Analysis | 17 |
| 1.4.2 Vibration and Damping | 17 |
| 1.5 Finite Element Analysis | 19 |
| 1.5.1 Non-Linear FEA | 20 |
| 1.6 Spin Testing | 20 |
| 1.6.1 Tub Blade | 20 |
| 1.6.2 Pocket Blade | 22 |
| 1.7 Discussion | 26 |
| 2. References | 28 |

List of Figures

| | | |
|----|--|----|
| 1 | Comparison of body force deformations for fluids and elastomers | 4 |
| 2 | Range of interest in rubbery elastic constants | 5 |
| 3 | Chip specimen in compression | 5 |
| 4 | Finite element model of chip/slip specimen | 7 |
| 5 | The growth in diameter of slip specimen depends on Poisson's ratio | 7 |
| 6 | Normalized axial compliance depends on chip length and Poisson's ratio | 8 |
| 7 | Complex shear modulus nomogram for PR 1564 | 9 |
| 8 | Specific volume versus pressure for Dyad 609 | 10 |
| 9 | Specific volume versus pressure for PR1546 | 10 |
| 10 | Dilatation versus pressure for PR1546 | 11 |
| 11 | Bulk modulus versus pressure for PR1546 | 12 |
| 12 | Poisson's ratio versus pressure for PR1546 | 12 |
| 13 | Volume versus temperature for PR1546 at selected pressures | 13 |
| 14 | Thermal expansion coefficient versus temperature for PR1546 at selected pressures | 14 |
| 15 | Photo of unassembled test blades | 15 |
| 16 | Cavity wall stress for viscostatic loading | 16 |
| 17 | Blade root and fastener location stress variation with spin rate | 16 |
| 18 | Stress in Cavity Wall for G=200 psi | 17 |
| 19 | Natural frequency variation with spin rate | 18 |
| 20 | Modal damping variation with spin rate | 18 |
| 21 | Tub blade configuration | 21 |
| 22 | Photo of front of viscoelastic tub blade | 21 |
| 23 | Tub blade results | 22 |
| 24 | Viscoelastic pocket blade schematic | 23 |
| 25 | Front side of the viscoelastic pocket blade | 23 |
| 26 | Measured vs. predicted strain measurements at the pocket middle | 24 |
| 27 | Measured vs. predicted strain measurements at the pocket outer edge | 25 |
| 28 | Comparison of mass adjusted predictions vs. measured results | 25 |
| 29 | Unspun frequency response functions comparing the response of the damped and undamped blade to PZT provided excitation | 26 |
| 30 | Frequency domain dynamic excitation results on the viscoelastic pocket blade | 27 |
| 31 | Time domain dynamic excitation results on the viscoelastic pocket blade | 27 |

List of Tables

| | | |
|---|---|----|
| 1 | Pocket configuration with a shear modulus of 1200 psi | 19 |
|---|---|----|

1. Properties of Viscoelastic Materials Under Centrifugal Loads

1.1 Summary

Hardware representative of viscoelastic damping material in a cavity in a spinning jet engine blade was investigated. Specimens representing jet engine fan blades were analyzed, designed, fabricated and spun to establish that elastomer filled cavities may be satisfactorily designed for in service high-g and thermal loading and satisfactorily analyzed using conventional finite element analysis. A spin rate of 7500 RPM at a radius of 16 inches was achieved which resulted in a g-level of 25,500. Some excitation and response vibration data during spin were acquired. Static strain readings were taken for the cavity walls.

1.2 Introduction

Augmentation of vibration damping in rotating blades of jet engines is of significant interest in order to enhance high cycle fatigue life. In most potential vibration damping applications, the achievement of damping of realistic hardware in a laboratory setting is reasonably easy; the accommodation of many other practical design, materials, manufacture, and service aspects can be challenging. Free layer damping surface coatings are susceptible to creep under centrifugal loading and erosion under airflow. Embedding the viscoelastic material in a cavity has a possibility of meeting these two design issues. The cavity/cavities can be located and the walls sized such that damping is provided in target vibration modes through shear strain energy in the viscoelastic material. An investigation by Gordon and Hollkamp [1] included a simplified analysis of hydrostatic pressure in a rigid wall container under body forces and indicated a great dependence on Poisson's ratio, whereas an analysis of flexible walls indicated significantly less pressure loading.

The primary concern is the hydrostatic-type loading due to the body forces in a high-g rotational field which can deform or rupture cavity walls. Strictly speaking, the term "hydrostatic" pertains only to fluids. In actuality, the damping, or energy dissipation, requires that a viscoelastic material be deformed in shear. As a first approximation, the VEM is considered to be a thermo-rheologically simple (trs) material. For vibratory energy dissipation, the VEM must be exercised in the transition region defined by a temperature and a frequency. The high-g spin loading occurs at static conditions, or zero reduced frequency. Under these conditions, the VEM behaves as if it were a rubbery material, where it possesses elastomeric properties. Elastomers are solids with values of elastic constants significantly lower than metals; they may be "nearly incompressible" or have a Poisson's ratio approaching a value of one-half. Under non-rotating conditions, one state of stress and strain exists; upon subjection to spinning conditions, the VEM will creep over time into another state of stress and strain. Provided a satisfactory design is achieved, this final state will

be one of small strains relative to the initial condition. Until some of the more obvious issues are resolved, it seems appropriate to analyze the polymer as a soft, linear elastic, homogeneous, isotropic solid undergoing small strains.

Because the damping material behaves as a viscoelastic material and creeps asymptotically into an elastomeric state under spin, the term "viscostatic" is used. A non-zero value for shear modulus is implied but values can be low; nothing is implied regarding the values of bulk modulus or Poisson's ratio. The "static" implies the equilibrium state after creep or relaxation processes have achieved asymptotic values. Finite element analysis (FEA) is used to predict the stress/strain situation under the viscostatic loading. The fact that the elastomeric behavior is characterized by "nearly incompressible" challenges the FEA. When the material is incompressible, the FEA is poorly conditioned numerically. Formulations exist which accommodate incompressible and nearly incompressible behavior when appropriate.

A major objective of this investigation was to determine the effects of the viscostatic type loading on possible cavity wall yielding, rupturing, or deformations which would degrade aerodynamic performance. Another objective was the measurement of vibration frequencies and damping during spin.

The elastic constants (shear modulus, youngs modulus, bulk modulus, and Poisson's ratio) elastomeric properties of the VEM were experimentally investigated. At this juncture, it seems that if practical levels of damping are to be achieved, the energy dissipation will be by means of the shear strain energy in the damping polymer. Consequently, the dynamic complex shear modulus is a significant design parameter, as it varies with temperature and the frequency of vibration. Because shear and volume strains are fundamentally different, it seems possible that the shear modulus might be little affected by the state of viscostatic pressure.

The high-g body forces must be reacted by the cavity bottom and/or walls. A sophisticated FEA is required to obtain values for predicted stresses. A single cavity configuration was analyzed and rejected because of fabrication expense. A "tub" and a two "pocket" configurations were analyzed, designed, fabricated and tested under spin.

1.3 Material Considerations

It is appropriate to analyze the polymer as a soft, linear elastic, homogenous, isotropic elastomeric solid undergoing small strains. Strength and failure investigations are not warranted under these conditions. The Poisson's ratio may asymptotically approach a value of one-half. For any elastic solid, it suffices to know values for any two of the elastic constants. If values for the youngs modulus E and Poisson's ratio ν are known, the shear modulus G and the bulk modulus B may be determined:

$$G = \frac{E}{2(1 + \nu)} \quad (1)$$

and

$$B = \frac{E}{3(1 - 2\nu)} \quad (2)$$

If values for B and G are known, the Young's modulus and the Poisson's ratio may be determined:

$$E = \frac{9BG}{3B + G} \quad (3)$$

and

$$\nu = \frac{E}{2G} - 1 = \frac{3 - 2G/B}{6 + 2G/B} \quad (4)$$

A function which expands the scale as Poisson's ratio approaches close to 0.5 may be defined which is numerically equal to the number of nines which follow the 0.4 in Poisson's ratio

$$n_\nu = -1 - \log(0.5 - \nu) \quad 0 < \nu < 0.5 \quad (5)$$

This function may be used in the range of values of Poisson's ratio less than 0.4, but no advantage is claimed for that region.

Using a finite element model, the shear modulus of an elastomer in a rigid cavity was progressively reduced to near zero, and the pressure distribution never approached the hydrostatic distribution. This can be explained qualitatively as follows. Consider a rigid wall cavity filled with a fluid. (See Figure 1). In a one-g body force field, the upper surface of an infinitesimal slice is ABC. Subjected to a high-g field, the upper surface of the slice is displaced to A'B'C', an amount depending on the bulk modulus. The fluid of course has a value of shear modulus equal to zero. Now a soft elastomer is substituted having the same bulk modulus and a very small shear modulus. Consider that strains are small and linear and that no ruptures occur. Under these conditions, the edges of the upper surface remain at points A and C. A layer of infinitesimal thickness is deformed to AB'C. This layer can only assume this shape if it both shears and elongates; the layer is subjected to both shear and bulk type of strains, definitely not bulk or volume change only. Any flexibility of the walls at A and C would have a substantial effect.

In the interest of establishing a practical range of values of elastic constants for an elastomer or rubbery asymptotic quantities relevant to the present investigation, several considerations are relevant. For isotropic materials, there are only two independent elastic constants. Shear modulus and bulk modulus have been chosen as the basic ones. The structural material chosen for the spin test blade is aluminum, for which the Young's modulus is taken as 10.0 msi and the Poisson's ratio as 1/3; the corresponding shear modulus is 3.75 msi and the bulk modulus is 10.0 msi. The isothermal bulk modulus of mercury is 3.59 msi (by comparison, that of water is 0.316

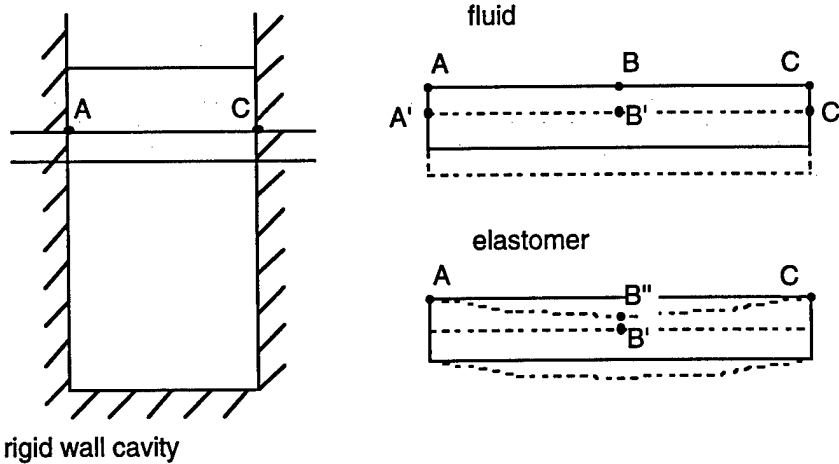


Figure 1: Comparison of body force deformations for fluids and elastomers

msi). These values are taken as approximate glassy (high frequency and/or low temperature or infinite value of reduced frequency) upper bounds for the corresponding properties of polymers or VEM's of interest. A practical lower limit of the rubbery (low frequency and/or high temperature or zero value for reduced frequency) Poisson's ratio is taken as 0.4, while the rubbery upper limit can theoretically approach 0.5 asymptotically. These quantities are not independent and are interrelated by well known equations. The region of interest is shown in Figure 2.

From measurements taken during this effort for VEMs/polymers under consideration, 500 ksi would be an upper limit for rubbery bulk modulus. Fluids have zero shear modulus. In the parametric study of the viscostatic type loading, a shear modulus of 1,000 psi and a bulk modulus of 100 ksi is somewhere near the center of interest; approximately 0.495 is the corresponding Poisson's ratio. This point is indicated on the Figure. If the rubbery value for shear modulus is greater than 10 psi and if that for bulk modulus is less than 500 ksi, it may be seen that Poisson's ratio is less than 0.49999 (i.e., four 9's). This fact and the experience of the present investigation with FEA lends great confidence to the efficacy of standard FEA codes.

A circular cylinder of rubber-like material, sandwiched between two rigid surfaces and bonded to them as in Figure 3, can be said to be in compression [4], although its behavior depends on the relative diameter and length. For a cylindrical specimen which has the aspect ratio of a pencil, it is well known that its extensional stiffness is given by

$$k = \frac{EA}{L} \quad (6)$$

This equation also applies for the slip interface specimen (ends are free to slip with respect to the end plates) regardless of dimensions. For a cylindrical specimen having an aspect ratio of a very thin pancake, the stiffness is given by

Bulk and Shear Modulus Range

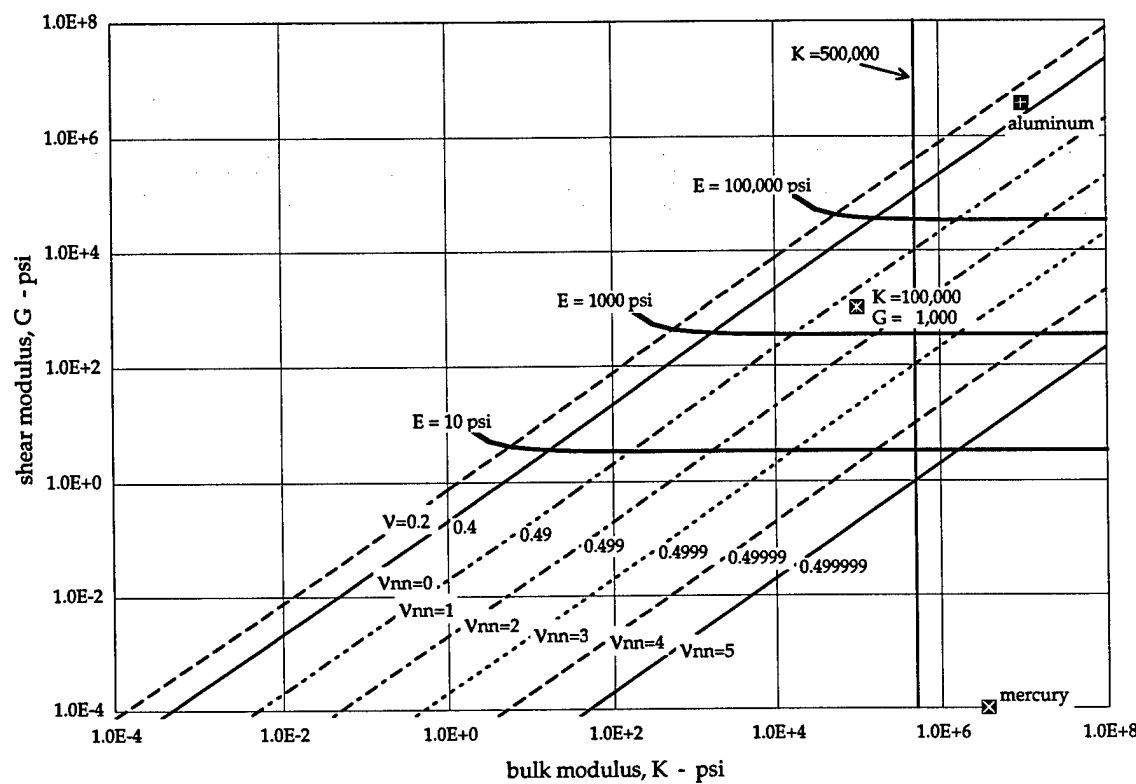


Figure 2: Range of interest in rubbery elastic constants

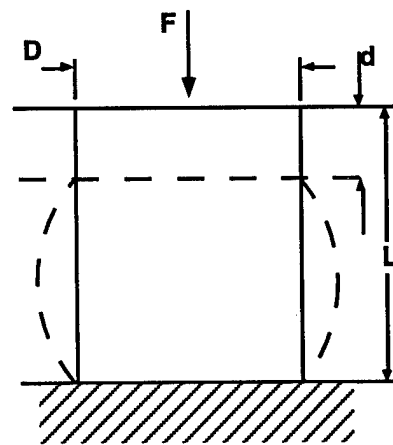


Figure 3: Chip specimen in compression

$$k = \frac{WA}{L} \quad (7)$$

where W is the longitudinal wave propagation modulus and is given by [4]

$$W = B + \frac{4G}{3} \approx B \quad (8)$$

The apparent modulus may be determined from a measured stiffness, k , or compliance, $1/k$:

$$E_a = \frac{kL}{A} \quad (9)$$

The apparent modulus is bracketed by

$$E < E_a < W \approx B \quad (10)$$

Chan et al. [2] and Sim and Kim [3] give several references for the static elastic case. They also extend the concept to the situation where the experimental results are based on measurement of frequency dependent vibration transmissibility results and aided in the analysis by FEA methods. In the present investigation, several materials were considered. A polymer, Courtaulds PR 1564, which was castable and which has elastomeric properties at room temperature and zero frequency was selected for incorporation into the spin test blade. Testing was performed on Courtaulds PR 1564, Courtaulds PR 1546, Ciba 6442, and Soundcoat Dyad 609.

In the present investigation, 3.0, 0.3, and 0.05-inch-long by 3.0-inch-diameter "poker-chip" or "chip" specimens (bonded to rigid end surfaces/plates which are also used to load the specimen in compression) were fabricated. For the chip specimens, the force and the change in length were measured. Also, 3.0-inch-diameter by 3.0-inch-long interfacial-slip, or "slip" (the ends were greased) specimens were fabricated. The force, the change in length, and the change in circumference were measured. The chip and slip type of specimens and their dimensions were chosen for their practicality and accuracy in determining values for the rubbery elastic constants.

1.3.1 Interfacial Slip

The bonded end surface of the cylindrical "poker chip" specimens prevents any radial displacement and results in wooden barrel like bulging. With a perfectly lubricated slip interface at the end plates, a specimen under compression will have a uniform radial displacement over the entire length. The apparent and the actual Young's modulus from this slip test are identical.[3] Furthermore, the radial compliance is dependent on the Poisson's ratio.

A finite element model of the 3-inch-diameter by 3-inch-long slip specimen, as shown in Figure 4, was generated and the axial compliance and the radial compliance computed for a range of Poisson's ratio.

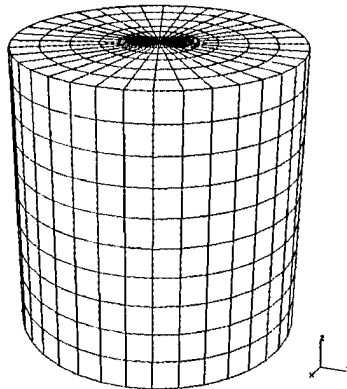


Figure 4: Finite element model of chip/slip specimen

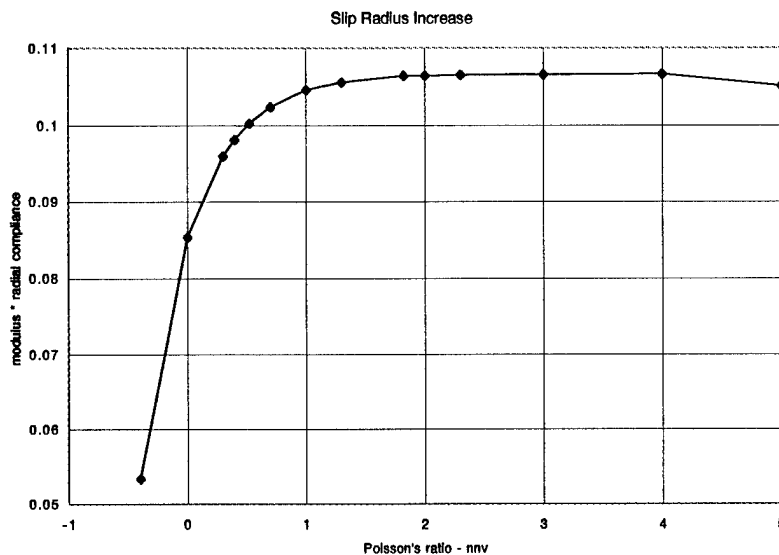


Figure 5: The growth in diameter of slip specimen depends on Poisson's ratio

The radial compliance times Young's modulus ($E * c_r$) is plotted in Figure 5 as a function of the Number of Nines in Poisson's Ratio. Between 4 and 5 nines, an artifact of the FEA may be observed.

Verification of the slip interface can be challenging. This method has been used successfully when three circumferential elongation hoop gages are used at different locations along the length. Care is taken to assure that the gage does not unduly deform the polymer during test at the circumferential line of contact and pressure. Furthermore, care must be taken to assure that there is a true slip interface, i.e., no sticking at the surface, which would give some barrel bulging. Vaseline Petroleum Jelly or other lubricants are used. Experimental data for two specimens each of different material resulted in approximately 0.4 for $E * c_r$, which is clearly an erroneous value. Facilities and equipment were not available for a ramp and hold type loading which would have been highly desirable; testing was performed at cyclic frequencies as low as 0.001Hz. Young's modulus was determined to be 541 psi for the 1564 and 4022 psi for the 6442.

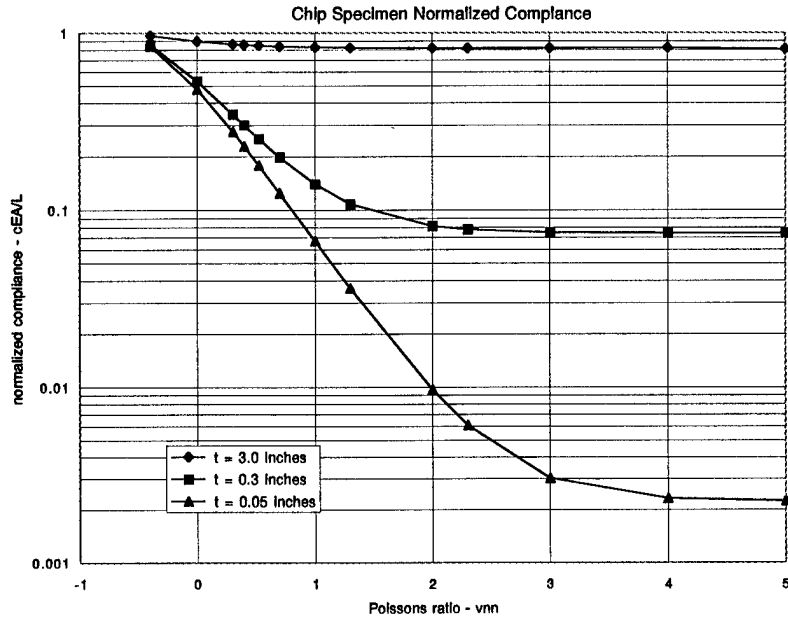


Figure 6: Normalized axial compliance depends on chip length and Poisson's ratio

1.3.2 Poker Chip

A “poker chip” is a cylindrical specimen with the ends bonded to plates which prohibit any radial deformation at the ends and which enable axial loading.

Two publications, Chan and Sim ([2] and [3]), have documented procedures for obtaining two viscoelastic properties thru a combination of testing and FEA. Vibration transmissibility tests were used in the references, but for the present investigation, only the rubbery elastic constants are of interest.

A finite element model of the 3 inch diameter chip specimens for each length (3.0, 0.3 and 0.05 inches) was generated and the axial compliance computed for a range of Poisson's ratio.

The quantity (axial compliance times Young's modulus times area divided by length) is plotted in Figure 6 as a function of the Number of Nines in Poisson's Ratio for each of the lengths.

Experimental axial compliance data from the 0.05 chip of 1564 indicates a Poisson's ratio of 0.48; the 0.3, 0.494. Data from the 0.05 chip of 6442 indicates a Poisson's ratio of 0.482. Facilities and equipment were not available for a ramp and hold type loading which would have been highly desirable; testing was performed at cyclic frequencies as low as 0.001Hz.

1.3.3 Complex Shear Modulus

The reduced frequency plot of complex valued shear modulus for Courtaulds PR1564 shows a maximum material loss factor of approximately 0.6 and a rubbery asymptotic

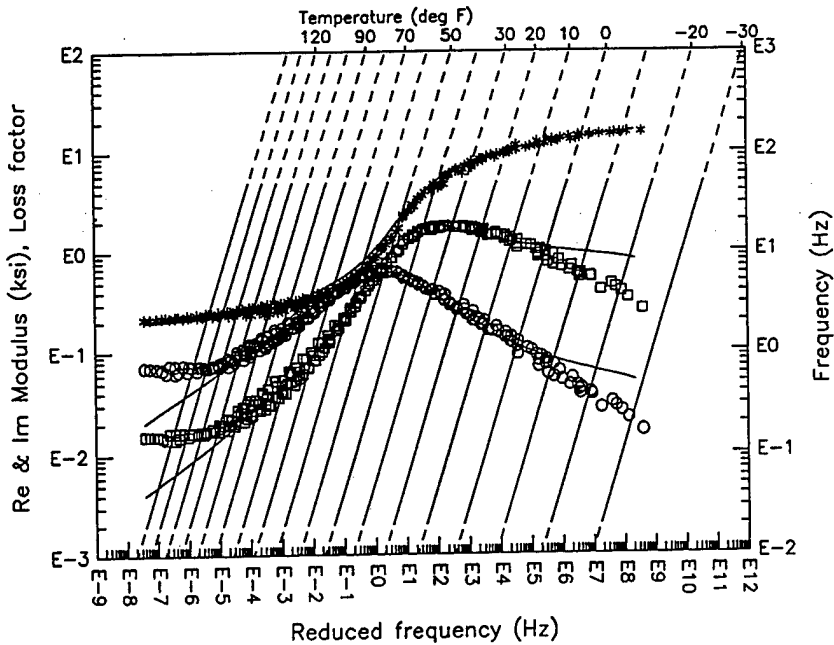


Figure 7: Complex shear modulus nomogram for PR 1564

value of approximately $G = 200$ psi (see Figure 7).

1.3.4 PVT Data and Analysis

For near static conditions, a pressure vessel test can be used where the sample material is exposed to a controlled hydrostatic pressure and a controlled temperature while the specimen volume change is measured. If a high accuracy system is used the pressure and volume change data can be used to calculate the VEM specimen bulk modulus. Dr. Zoller at the University of Colorado was engaged to test Soundcoat Dyad 609, which is a stiff material, and Courtaulds PR-1546, which is a soft material. The test apparatus is a Pressure-Volume-Temperature (PVT) device. The specimen is a one to two gram sample. The specimen is contained in a very thin cup and surrounded by a nearly incompressible liquid (mercury in this case). The cup is to ensure that the specimen is in a state of true hydrostatic pressure. The measurement and study of dimensional changes of matter may be termed dilatometry [5].

The data obtained from the PVT apparatus is the specimen volume as a function of pressure at various temperatures and is shown in Figures 8 and 9.

The set of Dyad 609 data is suspicious and is not considered further. Derived thermophysical parameters, such as the volume expansion coefficient, the isothermal compressibility, or the bulk modulus can be determined as a function of pressure and temperature. If the volume, V , can be expressed as a function of pressure, P , and temperature, T , the coefficient of volume thermal expansion is defined as

$$\beta(P, T) = 1/V(P, T) [\partial V(P, T) / \partial T]_p$$

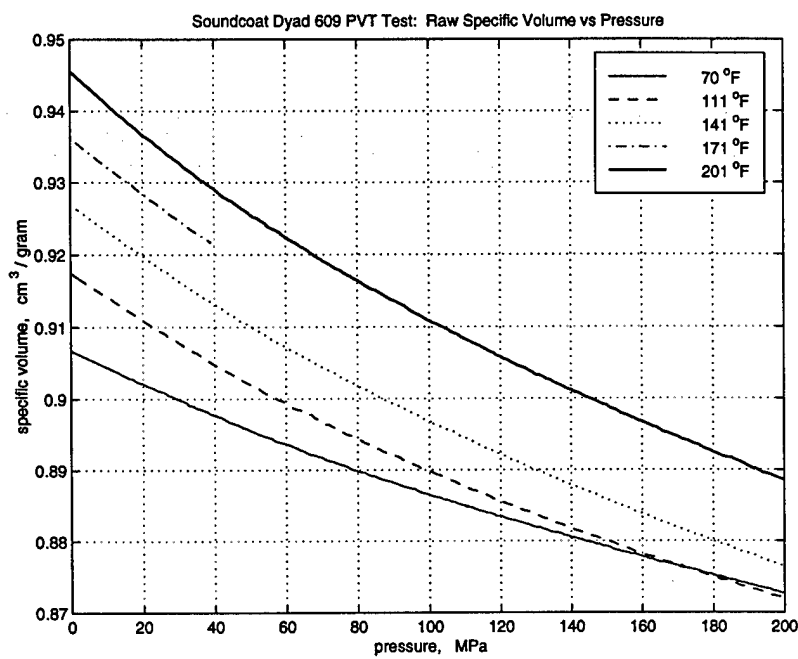


Figure 8: Specific volume versus pressure for Dyad 609

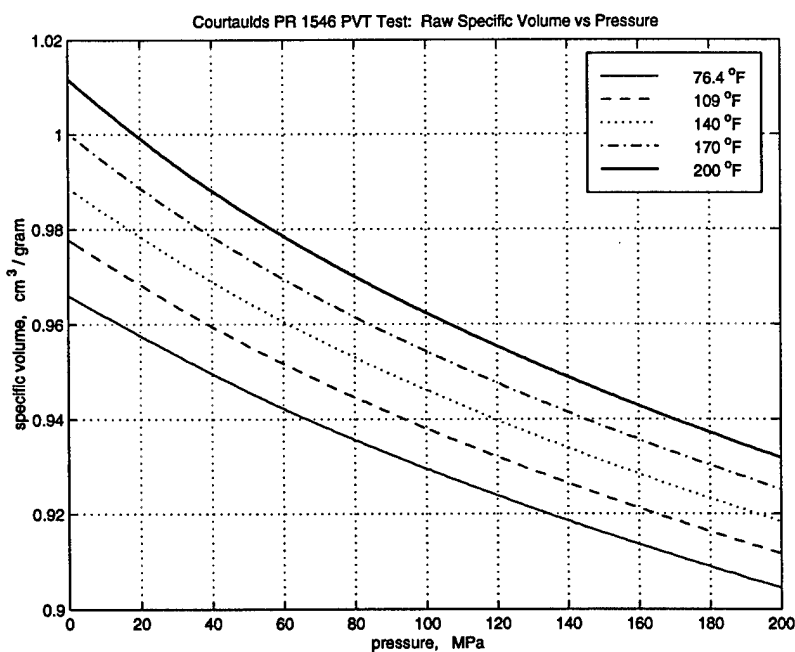


Figure 9: Specific volume versus pressure for PR1546

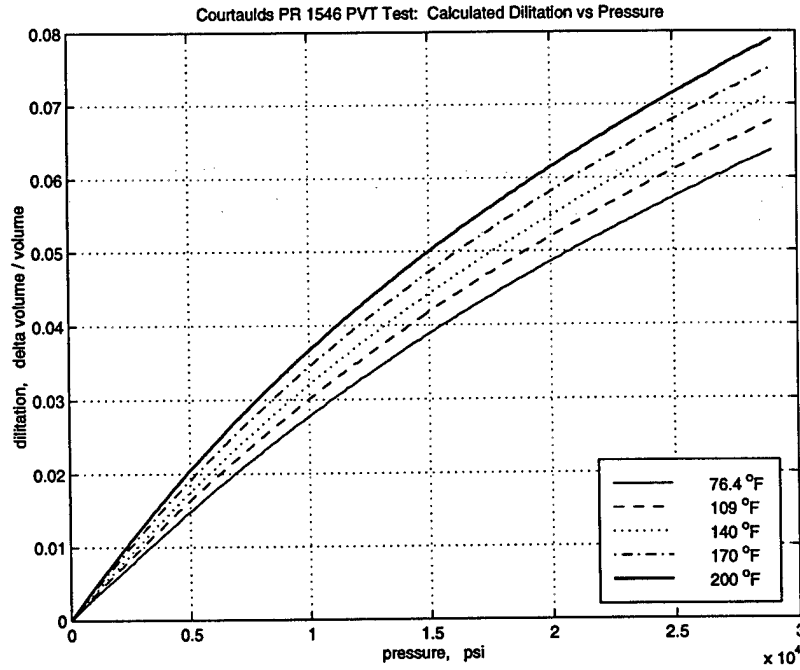


Figure 10: Dilatation versus pressure for PR1546

A coefficient of linear thermal expansion may be defined

$$\alpha(P, T) = 1/L(P, T) [\partial L(P, T) / \partial T]_p$$

where L is a linear dimension. For isotropic solids $\beta = 3\alpha$. The isothermal compressibility, a function of pressure and temperature, describes the relative volume change with pressure [5].

$$c(P, T) = -1/V(P, T) [\partial V(P, T) / \partial P]_T$$

The dilation (volume change divided by the initial volume) and then the bulk modulus

$$\frac{1}{K} = -\frac{1}{V} \frac{dV}{dP} \approx -\frac{1}{V} \frac{\Delta V}{\Delta P} \approx -\frac{1}{V_o} \frac{V - V_o}{P - P_o}$$

can be determined. Here the lowest pressure is taken as the reference as is the lowest temperature; consequently, the properties are based on a chord from the reference to a point rather than a tangent at the point (see Figures 10 and 11). The bulk modulus is seen to be both temperature and pressure dependent. It ranges from about 210 ksi to 460 ksi. This is consistent with other experimental data for soft, "nearly incompressible" elastomers. A reasonable upper bound for bulk modulus is 500 ksi.

An estimate for Poisson's ratio may be obtained from the bulk modulus from the figure when a value of 160 psi (taken from literature) is used for the shear modulus (see Figure 12).

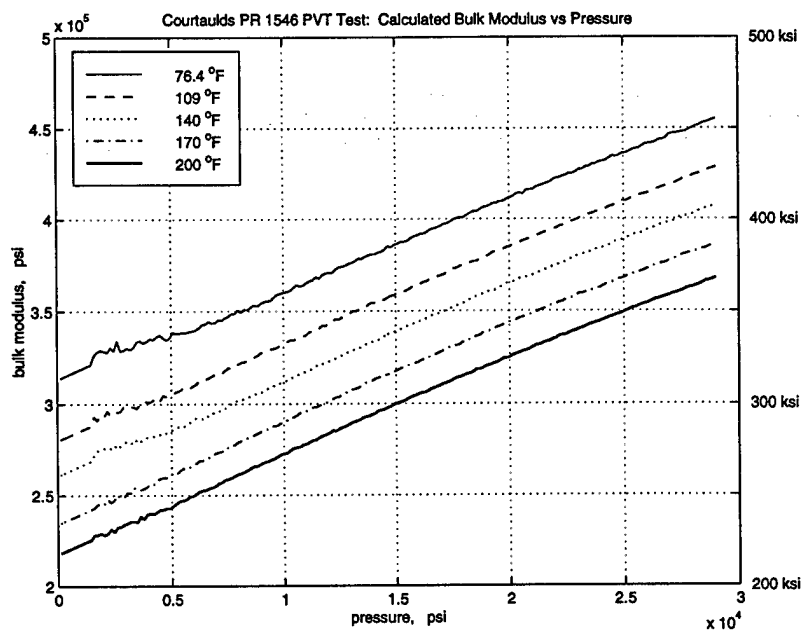


Figure 11: Bulk modulus versus pressure for PR1546

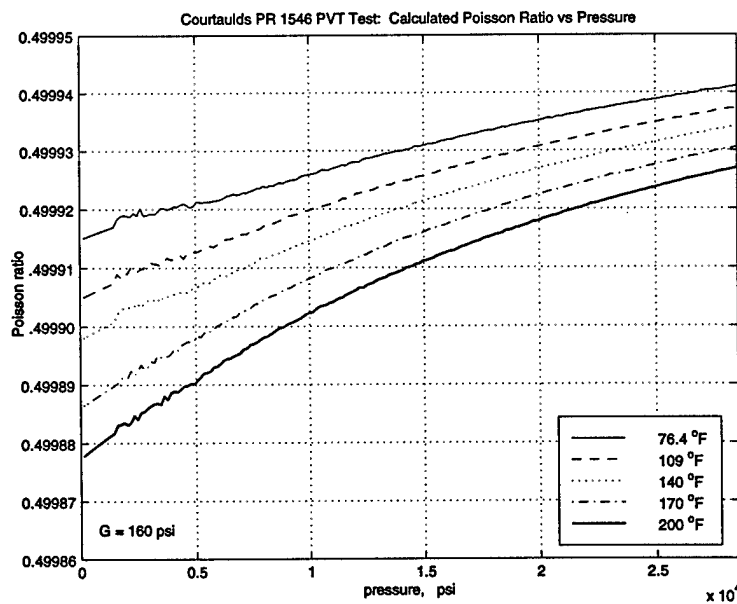


Figure 12: Poisson's ratio versus pressure for PR1546

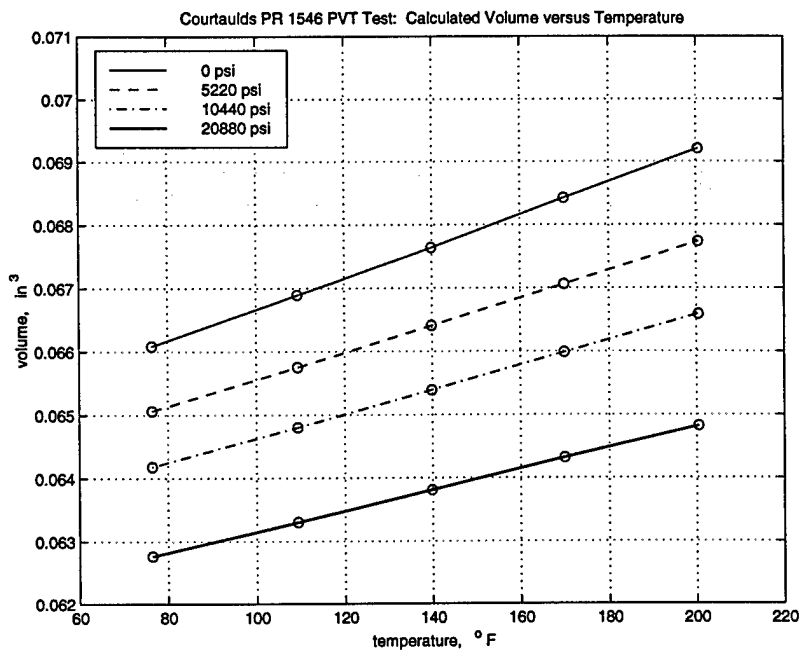


Figure 13: Volume versus temperature for PR1546 at selected pressures

The volume may be determined as a function of temperature for various values of constant pressure (see Figure 13) and the coefficient of thermal expansion calculated

$$C_{cte} = -\frac{1}{V} \frac{dV}{dT} \approx -\frac{1}{V} \frac{\Delta V}{\Delta T} \approx -\frac{1}{V_o} \frac{V - V_o}{T - T_o}$$

as a function of temperature and pressure. It varies between 2.5e-4 and 4e-4 in/in/F (see Figure 14).

For a linear material with constants independent of temperature and pressure, the volume change may be calculated using the following equation.

$$\Delta V = -\frac{V}{B} \Delta P + C_{cte} V \Delta T$$

This type of data with more appropriate processing is essential for investigations such as highly detailed analysis of PVT behavior of a polymer in a spinning cavity. However, in a practical application for damping, this level of sophistication is not necessary.

1.4 Experimental Blade Design

For purposes of reduced costs, aluminum was selected as the structural material for use in fabricating the experimental blade hardware. According to Mil-Hdbk-5, a value for tension ultimate strength of 80 ksi for 7075-T6 aluminum is appropriate. It is also

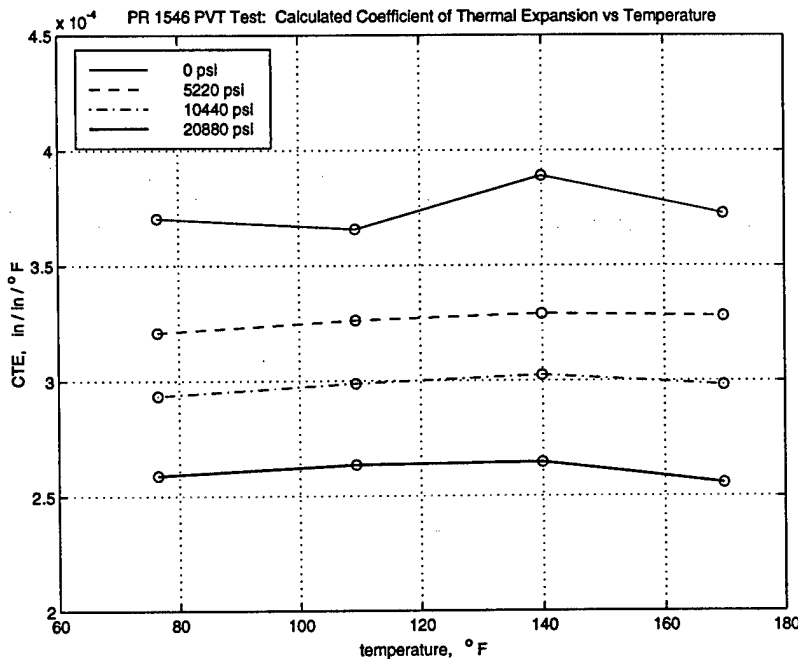


Figure 14: Thermal expansion coefficient versus temperature for PR1546 at selected pressures

appropriate to use a value of $2/3 * 80$ ksi = 53.33 ksi as a maximum predicted stress according to a credible analysis. This corresponds to a 5333 micro strain.

The “blade like” structure was selected to be an aluminum plate with a length to width aspect ratio of approximately 1.5 similar to USAF first stage fan blades. The Gordon-Hollkamp [1] arrangement served as a guideline. The blade did not have any curvature in order to minimize cost without compromising technological purposes.

Three configurations for VEM filled cavity blades were defined:

1. One-Pocket: A single pocket machined into a full solid blade with the cavity extending for the full chord. EDM (Electron Discharge Machining) was to have been used. Finite element analysis was performed on this one-pocket configuration with the solid blade being stainless steel and also aluminum. This configuration was rejected because of fabrication expense.
2. Pocket: A two pocket blade approximating one previously investigated [1] (see Figure 15). The polymer was 0.050 inch thick as were the cavity walls. This configuration was fabricated and spun up to 7500 RPM. The two “ice cube” pockets were cast full of polymer and a cover was bonded and bolted. This configuration possessed the highest modal damping levels.
3. Tub: A “tub” was mechanically fastened to the end of a solid blade. See Figure 15. The tub had a polymer which was 0.050 inch thick as were the cavity walls. The tub was full length (chordwise of the blade) machined and the ends were blocked. This configuration possessed a cavity wall arrangement

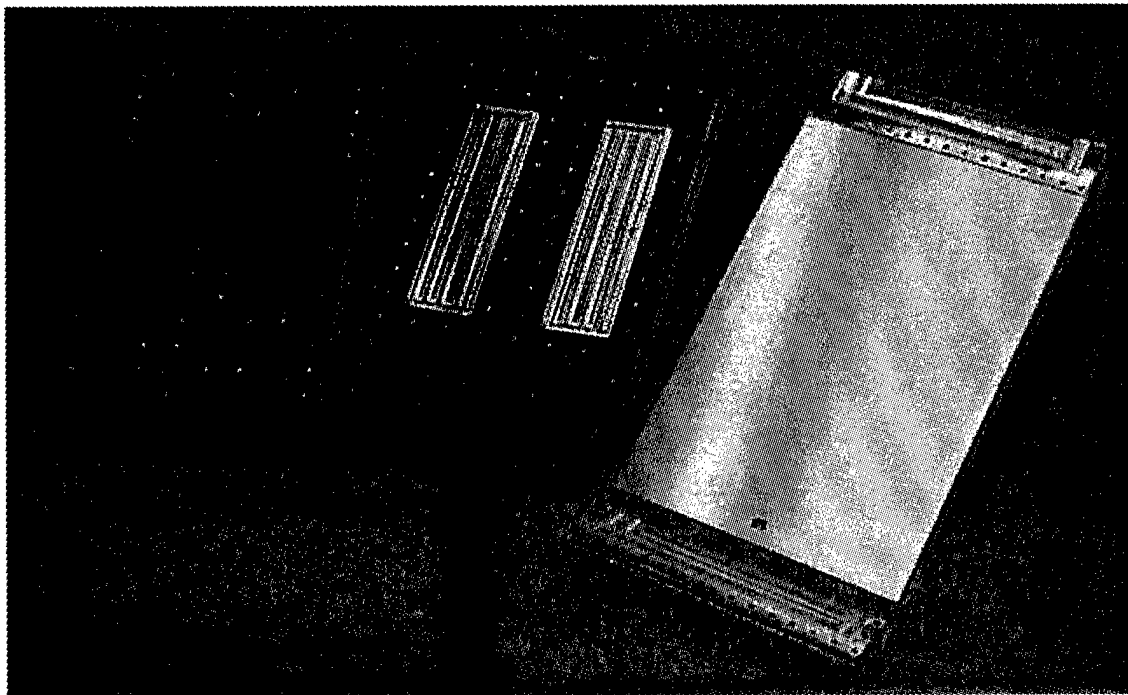


Figure 15: Photo of unassembled test blades

most amenable to analysis, fabrication and test. In the tub configuration, the polymer is very near the end of the blade where the viscostatic body forces are a maximum and the empty cavity wall stresses are a minimum.

The Pocket and the Tub configurations were fabricated and are shown in Figure 15.

It was decided to spin one blade at a time with a counterweight as balance in order to eliminate cross-talk between similar blades.

Several FEA of the tub were performed. In Figure 16, the stresses on the outside of the cavity wall are shown for 8000 rpm for a) empty cavity, b) cavity pressure only for viscoelastic material, c) cavity pressure only with hydrostatic fluid pressure, and d) both spin and viscostatic pressure. Stresses due to fluid and viscoelastic pressure only are seen to differ by three decades. This is a major finding of this investigation. The expected stress at 8000 rpm half way up the cavity wall is approximately 1000 psi. In Figure 17, the maximum stresses of concern are shown. The stress at two thirds of tension ultimate, or 53.3 ksi, is experienced at the root at 13 krpm. Stresses at the fasteners are much less. Thus it was considered safe to spin up to 13 krpm.

The results of a parametric FEA study are shown in Figure 18. The conditions are shear modulus of 200 psi and spin rate of 8000 RPM. The stress in the outside of the cavity wall is plotted for discrete values of Poisson's ratio as a function of the distance from the bottom of the tub. Note that the effect of Poisson's ratio changes both the shape and magnitude of the stress distribution. There is a significant jump between 0.49 and 0.499; other than the jump, the change is progressive. This lends credibility to the accuracy of the FEA up to five nine's. The tub walls flare out at the top to accommodate the mechanical fasteners. This causes a load eccentricity

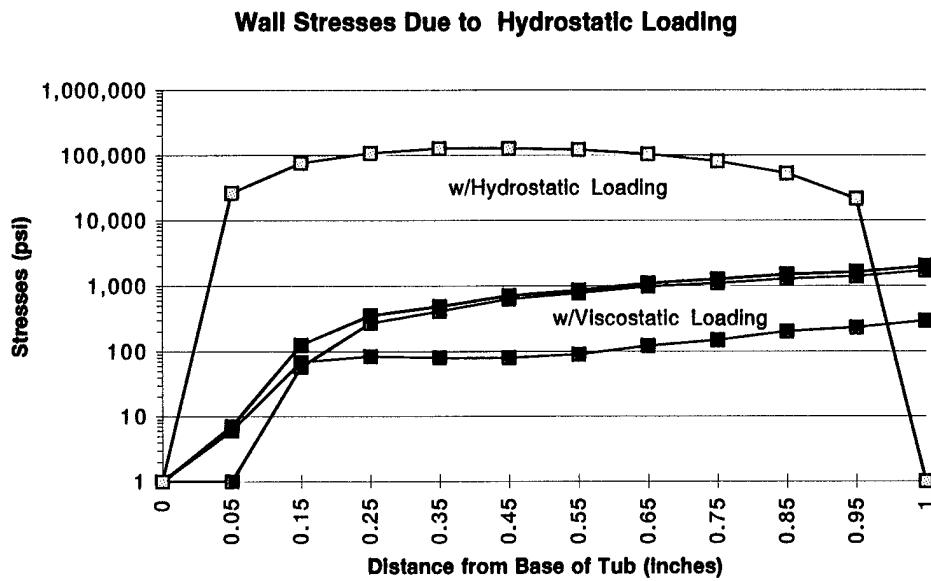


Figure 16: Cavity wall stress for viscostatic loading

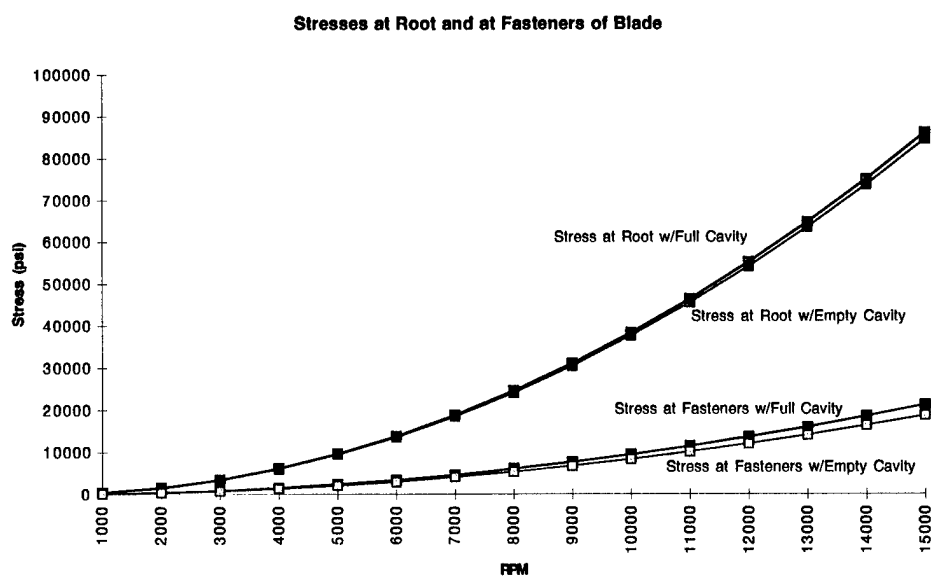


Figure 17: Blade root and fastener location stress variation with spin rate

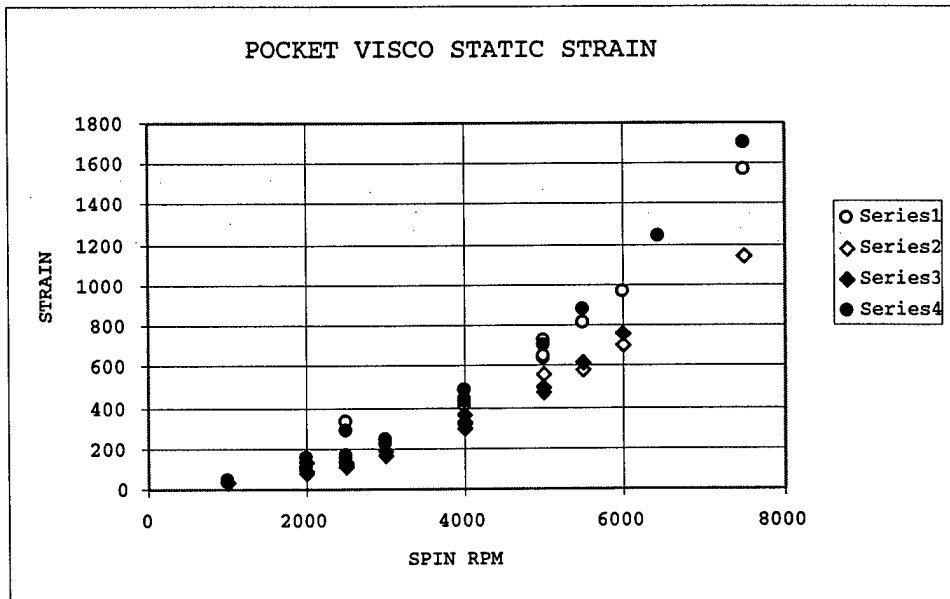


Figure 18: Stress in Cavity Wall for G=200 psi

which induces local bending and affects the pattern. The dependence on Poisson's ratio would suggest an effect of net volume change. Regardless, the stress levels are quite low and are easily accommodated during design.

1.4.1 Thermal Expansion Analysis

A finite element analysis of the pocket configuration was made with a value of the coefficient of thermal expansion of 0.0003 in/in/F, a shear modulus of 200 psi, a Poisson's ratio of 0.499, and a temperature increment of 500F. For this situation, stresses of 50 ksi were predicted in the cavity walls and the blade grew 0.040 inches in thickness. Both of these effects would be unacceptable; however, these effects would be greatly mitigated by a much thinner layer of polymer. A thinner layer is practical and also more desirable for damping purposes. The present thickness was chosen for economy of fabrication costs.

1.4.2 Vibration and Damping

Damping in all modes is desirable, but particular attention is due to the chordwise bending or "two stripe" modes as significant damping using historic approaches has been challenging.

Table 1 is for the pocket configuration with a shear modulus of 1200 psi. These values for the frequencies are plotted in Figure 19 together with the estimated dependence on spin rate. Using estimated values for material loss factor and dependence on spin rate, modal damping as a function of spin rate is plotted in Figure 20.

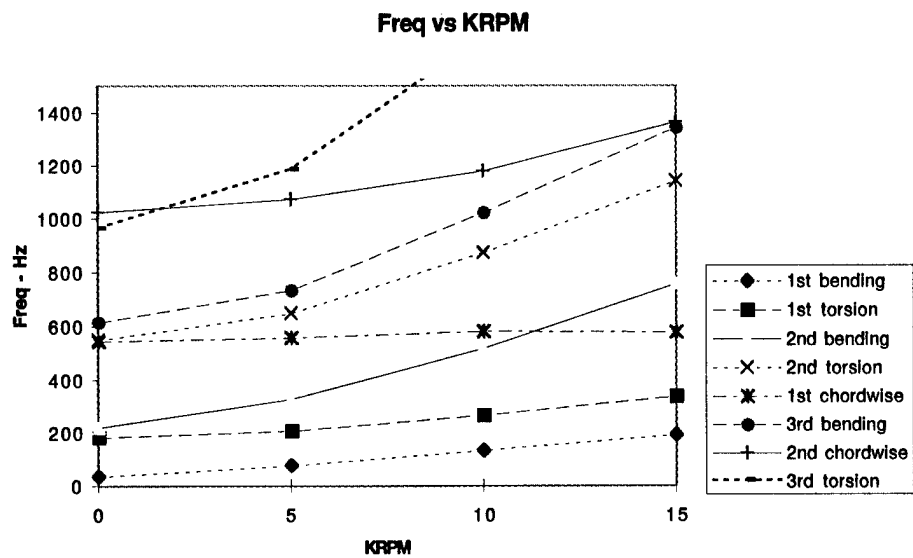


Figure 19: Natural frequency variation with spin rate

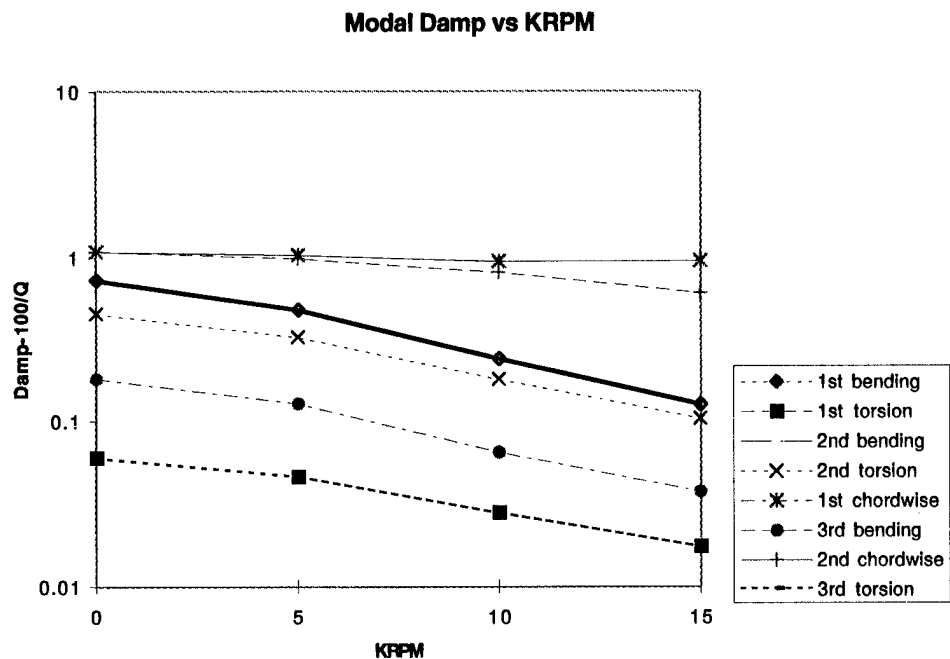


Figure 20: Modal damping variation with spin rate

| Mode | MSE | Frequency | Description |
|------|-----|-----------|---------------|
| 1 | 0.0 | 35 | 1B(bend) |
| 2 | 0.2 | 182 | 1T(torsion) |
| 3 | 0.0 | 219 | 2B |
| 4 | 3.6 | 544 | 1C(chordwise) |
| 5 | 1.5 | 548 | 2T |
| 6 | 0.6 | 614 | 3B |
| 7 | 2.4 | 965 | 3T |
| 8 | 3.6 | 1,024 | 2C |

Table 1: Pocket configuration with a shear modulus of 1200 psi

1.5 Finite Element Analysis

Specially formulated FEA codes exist for elastomers and associated difficulties. They can accommodate values of Poisson's ratio approaching one-half, very large strains of an elastomer, and stiff and soft materials adjoining each other. In the present investigation, there is no need for such sophistication.

One factor considered in the present investigation is the use of "nearly incompressible" materials in the cavity. Approaching incompressibility can sometimes result in numerical problems. In the limit, the material is incompressible, and all hydrostatic deformation is precluded. In that case, it is not possible to determine the complete state of stress considering strain only; which may be called an indeterminacy difficulty. Ill-conditioning results from division by a value which is extremely small. As the material nears incompressibility the stiffness matrix in the finite element analysis (FEA) becomes progressively more ill-conditioned. The poorly conditioned situation occurs as Poisson's ratio approaches a value of 0.5, which relates to the volume change of the polymer, not the basic physics or major effects on the cavity wall.

Another factor considered is that materials with radically different elastic properties are bonded together, i.e., the cavity wall material and the polymer. The dramatic change in properties causes a similar change in stress and energy levels in the materials. These factors sometimes give rise to difficulties in assessing accuracy of the FEA results.

In this investigation, FEA was used for sizing spin test blades, setting the spin test strategy, and a parametric study of effects of shear modulus, bulk modulus, and Poisson's ratio on cavity wall deflections. Higher order effects such as spin stiffening, stress softening, nonlinear stress strain curve, and hyperelastic elements were not used widely.

Since the FEA methods applicable to "nearly incompressible" materials are very complicated and are not routinely available, NASTRAN was used. Generally, a series

of values of Poisson's ratio approaching 0.5 were used whenever that was the case of interest. By this strategy, it is believed that the analysis was accurate to indicate trends.

1.5.1 Non-Linear FEA

A hyperelastic analysis was performed of the slip/chip specimens and compared with a standard FEA; the differences were practically indistinguishable. A piecewise linear analysis of a spinning polymer filled cavity was performed and compared with a conventional FEA; the differences again were indistinguishable.

1.6 Spin Testing

In addition to laboratory measurements, spin testing was performed to measure the effects of actual high centrifugal loads on viscoelastic material. The primary purpose was to measure viscostatic pressure effects on the cavity wall, while a secondary purpose was to measure dynamic behavior during spin. Two different blade geometries were tested. All were 8.0" wide, 13.25" long and 0.150" thick. The lower 1.25" was held in a clamped boundary condition, giving an effective length of 12.0" or an aspect ratio of 1.5, similar to fan blades. All blades were made from 7075-T6 aluminum and were 0.150" thick once assembled. Testing was performed in spin pit L-36 at the Hudson, Massachusetts facilities of Test Devices, Inc.

1.6.1 Tub Blade

The so-called tub configuration is specialized for the study of high centrifugal loads on viscoelastic material. The VEM (PR 1564) was cast in place in a pocket 1.125" long, 7.25" wide and 0.050" thick at the outer edge of the blade. It was cast in a tub-like end fixture that was then epoxied and bolted to the base blade. This configuration is shown in Figure 21. The blade was instrumented with 4 strain gages (type SK-06-062AP-350 from the Micro-Measurements Division of the Measurements Group, Inc.) as shown in Figure 22, with strain gages 1 & 2 placed at the root at the outer edges of the blade to measure the maximum static strain that was expected near these locations. Strain gages 3&4 are placed along the plate centerline as far towards the outer radius as possible on the tub cavity. These locations were chosen to measure the static strain of the viscoelastic tub container as it was rotated.

The blade was tested to its full rated speed, 7500 RPM, with no evidence of yielding in the pocket. This speed induced over a 25,000 g-level loading in the viscoelastic material. Instrumented measurements were made at lower speeds of up to 3500 RPM. The results and their correlation to predictions are shown in Figure 23. As can be seen the results agree well with predictions. The available data from all three tests is provided upon the same plot. The source of the scatter of results (primarily at 2500 RPM's) is unknown at this time.

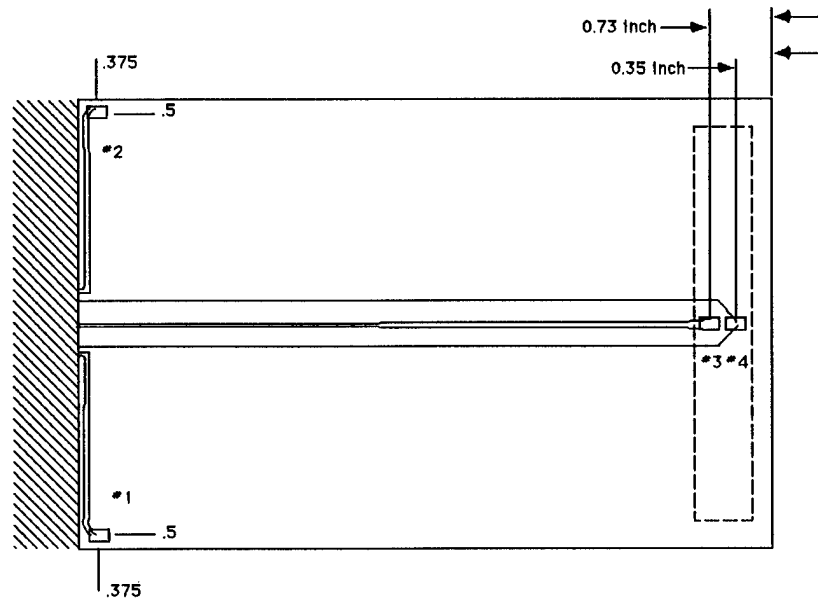


Figure 21: Tub blade configuration

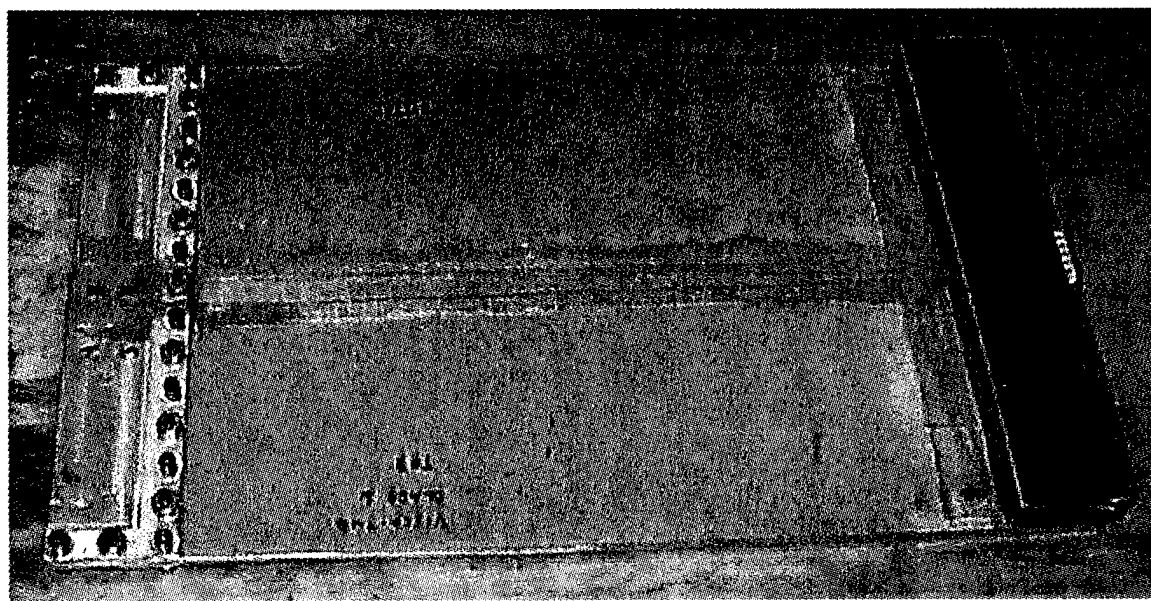


Figure 22: Photo of front of viscoelastic tub blade

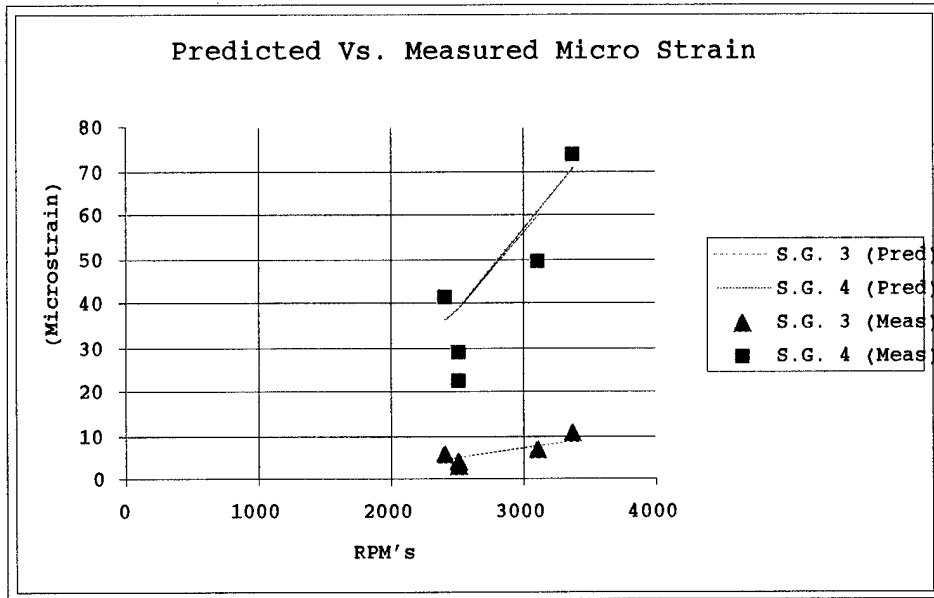


Figure 23: Tub blade results

1.6.2 Pocket Blade

This blade was designed to study the capability of VEM damping to address chordwise bending modes as well as enable measurements of static strain while under spin. The overall configuration of the blade is shown in Figure 24. The blade itself consisted of two thin plates, one 0.100" thick and the other 0.050" thick. The thicker base plate had two 0.050" deep pockets hollowed out to allow placement of the VEM which was cast in place. The top plate had the same basic geometry and bolting pattern as the base plate. For spin testing, one pocket was filled with PR 1564 and the other pocket was left empty. The plates were then epoxied together using Dexter Hysol 9330.30 and bolted for additional security in case of epoxy separation. The assembled flat blade was then instrumented with seven strain gages and 1 set of 2 chordwise Lead Zirconate Titanate (PZT) patch excitors (ACX Quickpack QP20W) epoxied onto the top and bottom of the blade. The piezo patches were oriented to maximize excitation of the chordwise bending modes and bonded to the blade with the same 9330.30 epoxy. This epoxy was chosen as it was the only one to survive earlier spin tests of patches with three different epoxies to survive ultimate spin speed with no failures. Arrangement of the pockets, the excitation PZT patches, and strain gage placement is given in Figure 24. A photograph of the finished hardware is reproduced in Figure 25.

After initial testing in the laboratory to determine unspun dynamic behavior and compare it to an otherwise identical blade with no viscoelastic treatment, the blade was balanced with its hub and counter-balance and installed in the spin pit. The blade was spun up in 2500 RPM steps from 0 to 7500 RPM as planned. Static strain was measured at these intervals and the blade was spun back down to zero. A second series of measurements were done in 1000 RPM steps from 0 to 5000 RPM with additional tests at 2500 and 5500 RPM. The results were consistent with one

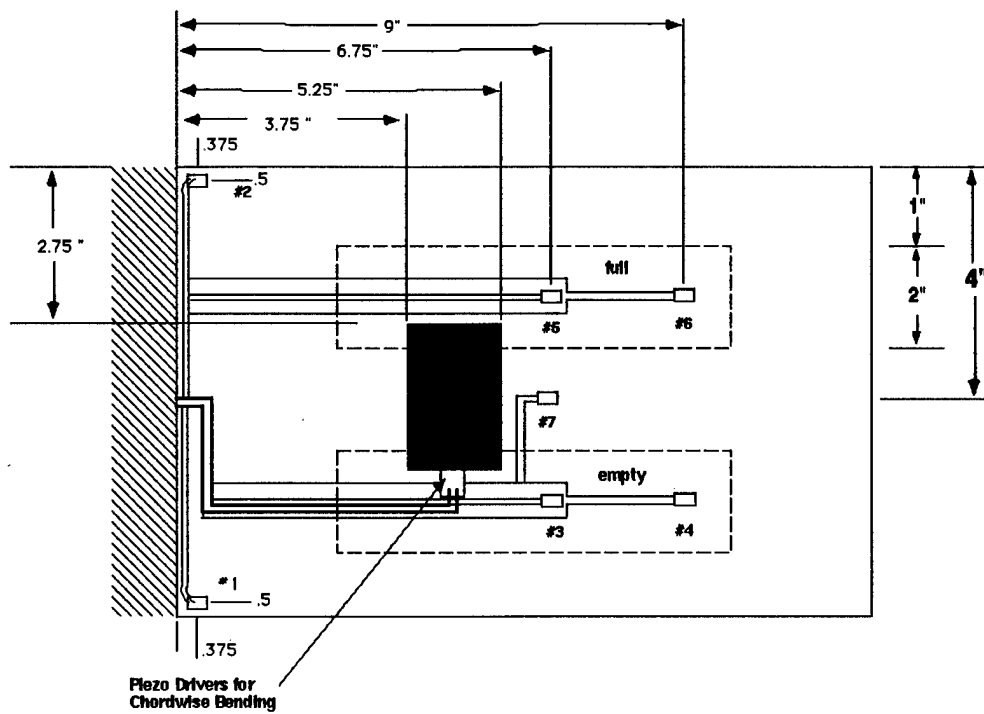


Figure 24: Viscoelastic pocket blade schematic

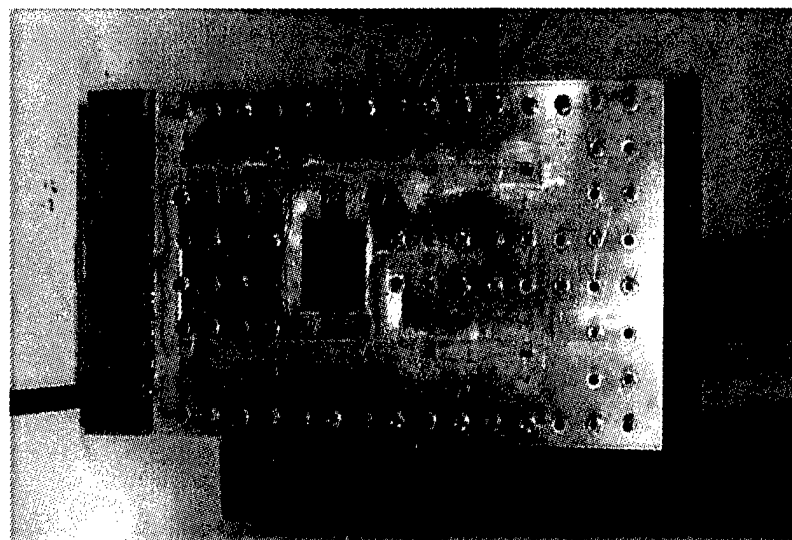


Figure 25: Front side of the viscoelastic pocket blade

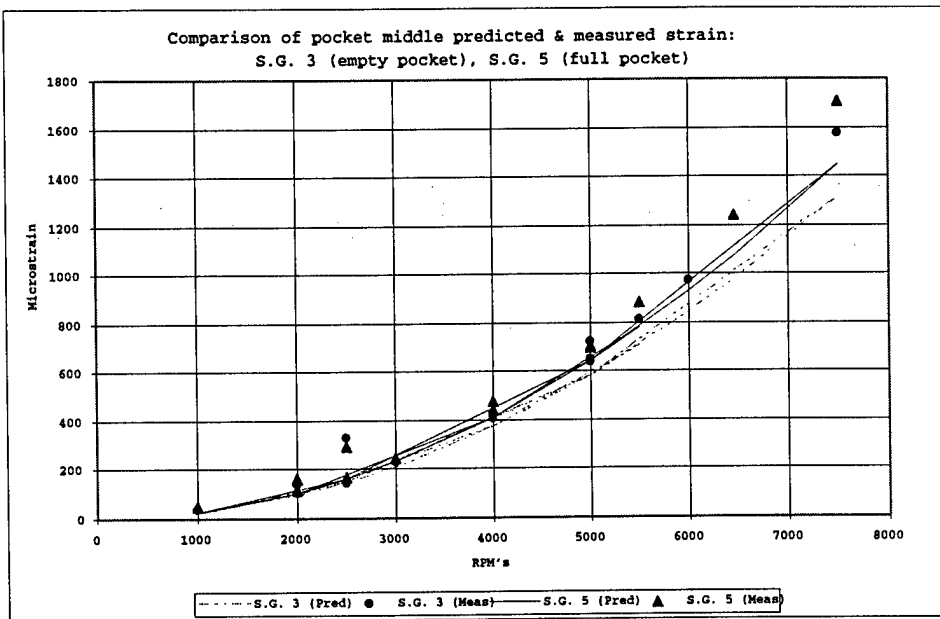


Figure 26: Measured vs. predicted strain measurements at the pocket middle

another and agreed in regards to trends with finite element modeling as shown in Figures 26 and 27. It can be seen that all strain gages read consistently higher than the predictions. This discrepancy is most likely due to the fact that the predictions were made with a model that did not include the numerous connector masses. Shown in Figure 28 is a comparison of the measured results and mass adjusted predictions. (17% added mass for S.G. 3&5 and 30% added mass for S.G. 4&6). With these adjustments, the agreement is quite good but appears to indicate a slightly greater dependence on RPM than predicted.

Despite these discrepancies, it can be seen that the measured strain results follow the same trends predicted in the analysis. Strain gages over the full pocket read slightly more strain than those over an empty pocket.

It was also attempted to measure the dynamic response of the blade due to excitation provided by the PZT chordwise actuators. Initial testing in the laboratory to determine baseline behavior established that the design did result in significant damping for the chordwise bending modes (at 430 and 680 Hz), as compared to measurements made on an identical blade with no damping treatment (Figure 29). It was hoped that the presence of this damping could also be demonstrated under spin conditions.

Due to a high level of cross talk between the PZT's and strain gages (the source of which is still under investigation), this proved difficult. Frequency response function's (FRF) were generated by exciting the PZT sets, and thus the blade, with a burst of pseudorandom band-limited noise of short duration and averaging the resulting blade dynamics as measured with the strain gages (See Figure 30). The higher level of cross talk caused by continuous excitation was reduced in this method. The cross talk was reduced enough so that by coupling the measured data with estimates from

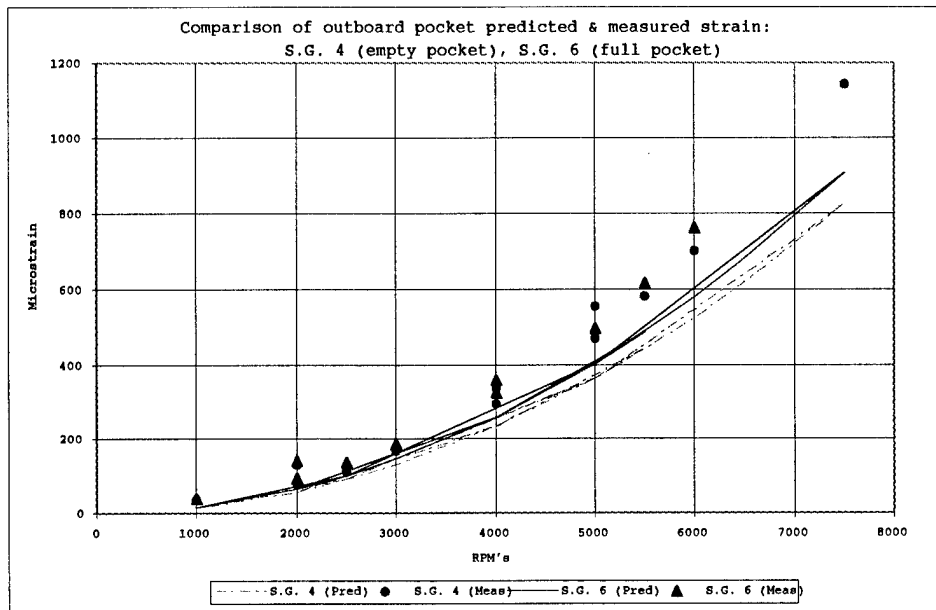


Figure 27: Measured vs. predicted strain measurements at the pocket outer edge

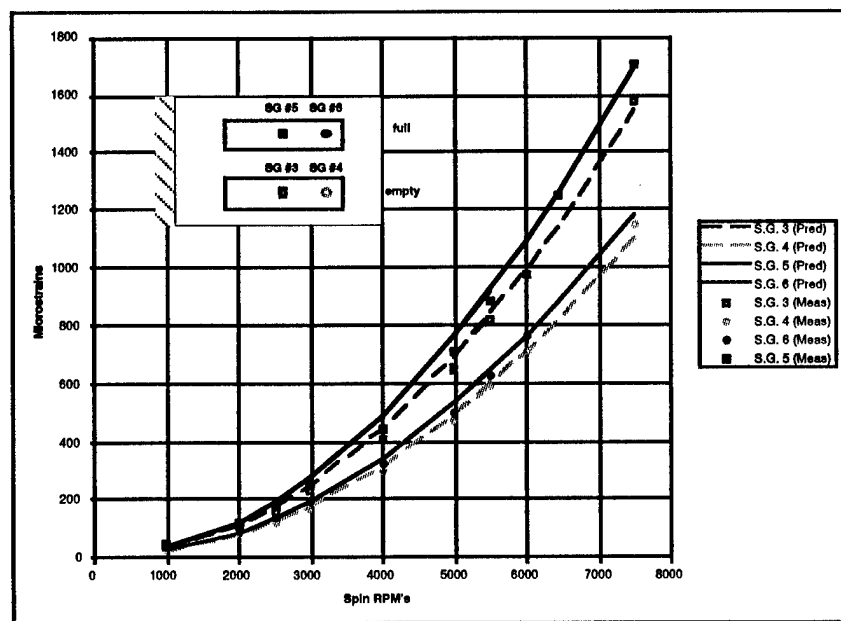


Figure 28: Comparison of mass adjusted predictions vs. measured results

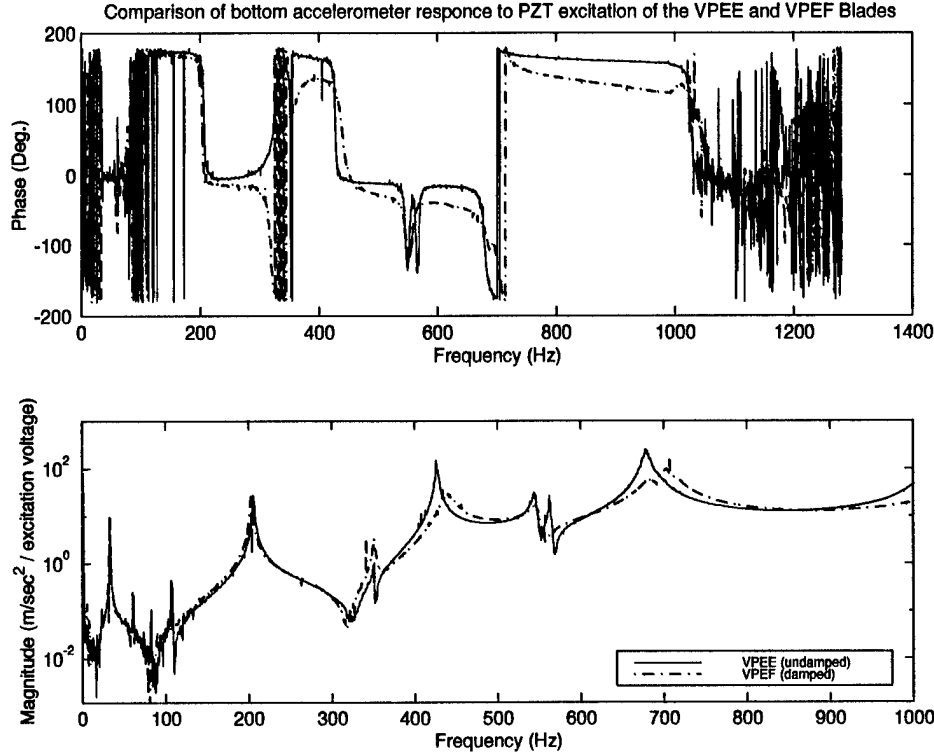


Figure 29: Unspun frequency response functions comparing the response of the damped and undamped blade to PZT provided excitation

the FE design model it was possible to extract several of the blade's lower natural frequencies. For one of these it also proved possible to excite the mode with a pure sine wave allowing measurement of the cross-talk free ringdown after halting excitation (Figure 31). No significant damping is present in this mode at 210 Hz though and it was not possible to identify the higher order chordwise bending modes due to the still present cross talk.

1.7 Discussion

A polymer filled cavity with polymer as far as 16 inches from the axis of rotation was spun at 7500 RPM giving a g-level of 25,500 and correlating well with FEA predictions (within 15 percent). According to the predictions, much higher rpm/g-levels are achievable with this design. An analysis of thermal expansion indicated that for this particular design, temperature rise would be limited to a few hundred degrees; however, a thinner layer of polymer would have much greater thermal capability.

Some dynamic data during spin of vibration excitation and sensing were obtained. This demonstrated the basic feasibility of the instrumentation including the slip rings. Further consideration of compatibility of the excitors and sensors, the shielding, etc of the set-up is indicated.

Finite element analysis of 5 different models were performed. In all of these, a

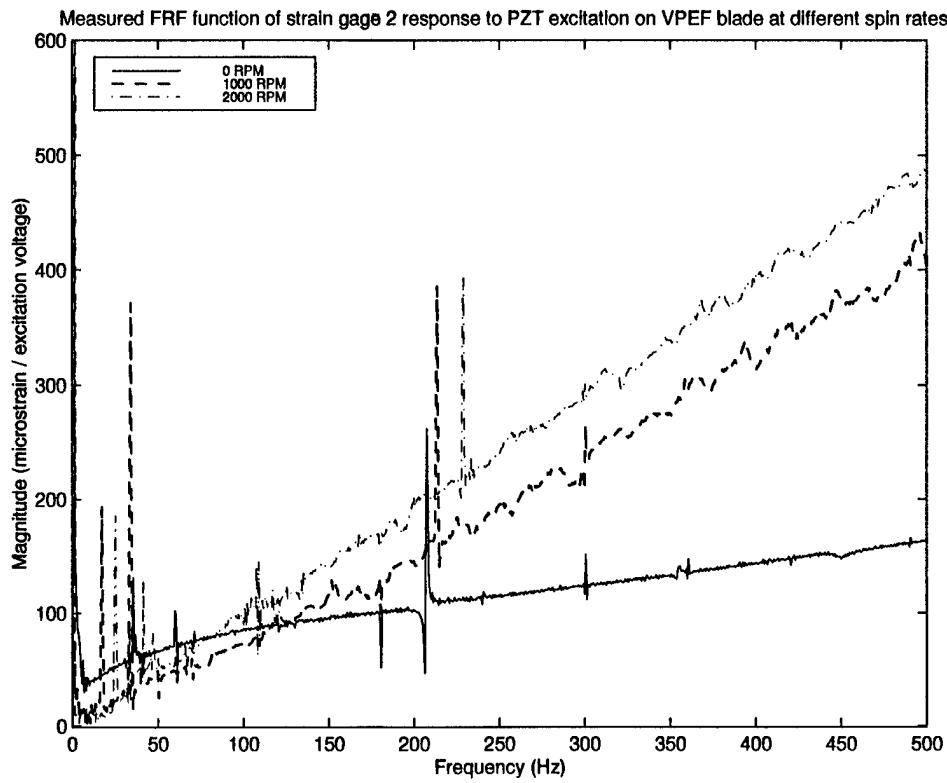


Figure 30: Frequency domain dynamic excitation results on the viscoelastic pocket blade

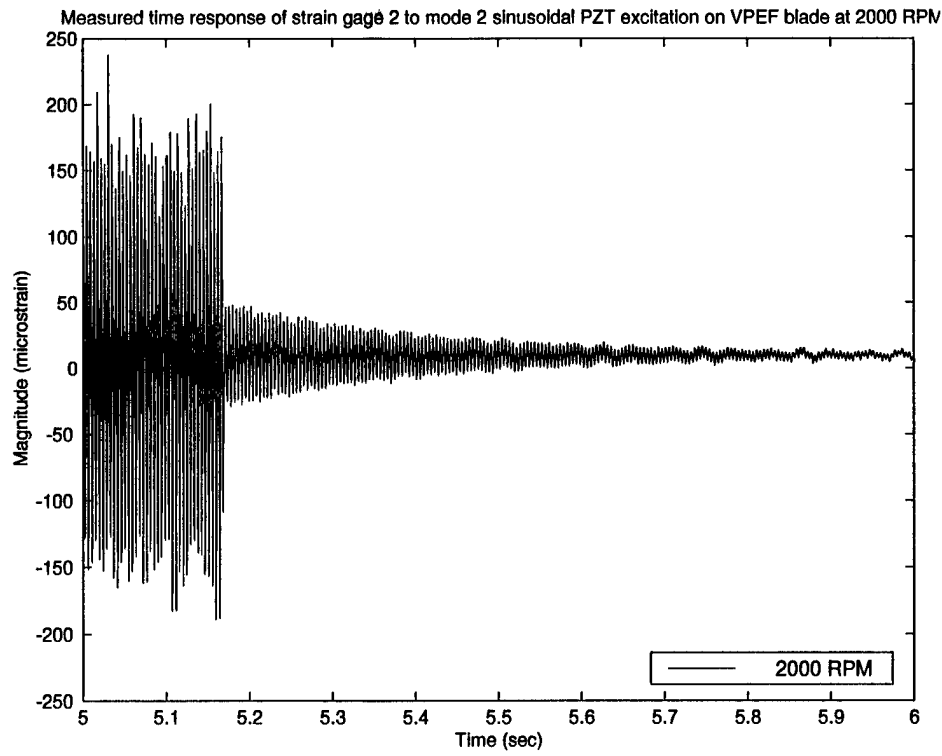


Figure 31: Time domain dynamic excitation results on the viscoelastic pocket blade

range of Poisson's ratio was included. No questionable results were observed out to 0.49999; at 0.499999, the slip results showed a small error. The 0.49999 probably covers practical materials.

2. References

- [1] R.W. Gordon and J.J. Hollkamp, "A comparison of damping treatments for gas turbine blades," SPIE Smart Structures and Materials Conference, 1995.
- [2] Y.W. Chan, S. Oyadiji, G. Tomlinson, & J. Wright, "Predicting the vibration characteristics of elements incorporating incompressible and compressible viscoelastic materials," SPIE Vol. 2445 Smart Materials and Structures, pp. 293-303, 1995.
- [3] S. Sim & K.J. Kim, "A Method to Determine the Complex Modulus and Poisson's Ratio of Viscoelastic Materials for FEM Applications," J. of Sound and Vibration, Vol. 141, no. 1, pp. 71-82, 1990.
- [4] J. Snowdon, "Vibration and Shock in Damped Mechanical Systems," Wiley, 1968.
- [5] P. Zoller, Dilatometry, pp. 131-141, "Polymers: Polymer Characterization and Analysis," ed. J.I. Kroschwitz, Wiley, 1990.

copies are being forwarded. Indicate whether Statement A, B, C, D, E, F, or X applies.

Title: Properties of Viscoelastic Materials Under Centrifugal Loads

DISTRIBUTION STATEMENT A:

APPROVED FOR PUBLIC RELEASE: DISTRIBUTION IS UNLIMITED

DISTRIBUTION STATEMENT B:

DISTRIBUTION AUTHORIZED TO U.S. GOVERNMENT AGENCIES ONLY; (Indicate Reason and Date). OTHER REQUESTS FOR THIS DOCUMENT SHALL BE REFERRED TO (Indicate Controlling DoD Office).

DISTRIBUTION STATEMENT C:

DISTRIBUTION AUTHORIZED TO U.S. GOVERNMENT AGENCIES AND THEIR CONTRACTORS; (Indicate Reason and Date). OTHER REQUESTS FOR THIS DOCUMENT SHALL BE REFERRED TO (Indicate Controlling DoD Office).

DISTRIBUTION STATEMENT D:

DISTRIBUTION AUTHORIZED TO DoD AND U.S. DoD CONTRACTORS ONLY; (Indicate Reason and Date). OTHER REQUESTS SHALL BE REFERRED TO (Indicate Controlling DoD Office).

DISTRIBUTION STATEMENT E:

DISTRIBUTION AUTHORIZED TO DoD COMPONENTS ONLY; (Indicate Reason and Date). OTHER REQUESTS SHALL BE REFERRED TO (Indicate Controlling DoD Office).

DISTRIBUTION STATEMENT F:

FURTHER DISSEMINATION ONLY AS DIRECTED BY (Indicate Controlling DoD Office and Date) or HIGHER DoD AUTHORITY.

DISTRIBUTION STATEMENT X:

DISTRIBUTION AUTHORIZED TO U.S. GOVERNMENT AGENCIES AND PRIVATE INDIVIDUALS OR ENTERPRISES ELIGIBLE TO OBTAIN EXPORT-CONTROLLED TECHNICAL DATA IN ACCORDANCE WITH DoD DIRECTIVE 5230.25, WITHHOLDING OF UNCLASSIFIED TECHNICAL DATA FROM PUBLIC DISCLOSURE, 6 Nov 1984 (Indicate date of determination). CONTROLLING DoD OFFICE IS (Indicate Controlling DoD Office).

This document was previously forwarded to DTIC on _____ (date) and the AD number is _____

In accordance with provisions of DoD instructions, the document requested is not supplied because:

It will be published at a later date. (Enter approximate date, if known).

Other. (Give Reason)

DoD Directive 5230.24, "Distribution Statements on Technical Documents," 18 Mar 87, contains seven distribution statements, as described briefly above. Technical Documents must be assigned distribution statements.

Gordon Negaard
Print or Type Name

Per E-mail with Gordon Negaard 937-255-6688
Authorized Signature/Date 3/26/99 RL Telephone Number